SOBOLEV GRADIENT TYPE PRECONDITIONING FOR THE SAINT-VENANT MODEL OF ELASTO-PLASTIC TORSION

ISTVÁN FARAGÓ AND JÁNOS KARÁTSON

(Communicated by Lubin Vulkov)

Abstract. In this paper a suitable Laplacian preconditioner is proposed for the numerical solution of the nonlinear elasto-plastic torsion problem. The aim is to determine the tangential stress in cross-sections under a given torsion, for which the physical model is based on the Saint Venant model of torsion and the single curve hypothesis for the connection of strain and stress. The proposed iterative solution of the arising nonlinear elliptic problem is achieved by combining the advantages of Laplacian preconditioners with the qualitatively favourable aspects of the strong formulation. Error estimate is given for the convergence of the method. Finally, a numerical example is given.

Key Words. Elasto-plastic torsion; nonlinear elliptic problem; iterative solution; Laplacian preconditioner.

1. Introduction

The investigation of the elasto-plastic torsion of a hardening rod has a great practical importance in mechanics and its theoretical background has been widely analysed (see, e.g., [11, 12]). The mathematical formulation of this problem leads to nonlinear differential equations. The most frequently used numerical methods that arise in this context are the finite difference and finite element methods [20, 23]. The solution of the obtained system of algebraic equations is generally found by some iterative method. The crucial point in the solution of these systems is most often preconditioning. Namely, since the condition number of the Jacobians of these systems tends to infinity when discretization is refined, therefore a suitable nonlinear preconditioning technique has to be used to achieve a convenient condition number [2].

In this paper the behaviour of the tangential stress is studied under the elasto-plastic torsion of a hardening rod based on the following model [12]: the cross-sections experience rigid rotation in their planes and are distorted in the direction of the z-axis (this is the Saint Venant model), further, the intensity of the stress is a strictly increasing function of that of the strain under the hardening condition. The arising mathematical model is a quasilinear elliptic boundary value problem of divergence form, in which nonlinearity comes from the stress-strain function.

As mentioned above, the main point in the numerical solution of the arising elliptic problem is preconditioning. A general efficient way to provide a suitable

preconditioner is the Sobolev gradient approach, developed by Neuberger for least-square methods [21, 22], which relies on using the Sobolev inner product. A strongly related kind of preconditioning is using the discrete Laplacian as preconditioner (see e.g. [7, 25]). These preconditioning methods benefit by the fast solvers available for the Laplacian, also involving general domains via the fictious domain approach (see also [25]). The Sobolev gradient technique points to the infinite-dimensional generalizations of iterative methods, which go back to Kantorovich [13] and have undergone extensive development. The authors' investigations include the gradient method for non-differentiable operators in a Hilbert space [14], and we underline that the Sobolev space background helps us in constructing effective natural preconditioners [3, 10, 21].

The Sobolev gradient approach yields a gradient (steepest descent) iteration in Sobolev space which reduces the solution of the nonlinear equation to the sequence of auxiliary linear Poisson problems. The numerical solution of these auxiliary linear problems by a suitable finite element method yields the gradient–finite element method (GFEM) introduced by the authors in [9]. This method combines the above mentioned advantages of Laplacian preconditioners with the qualitatively favourable aspects of the strong formulation. The GFEM is proposed in the present paper for the numerical solution of the elasto-plastic torsion problem. The main advantages of the GFEM are an easy algorithmization and preserving the ellipticity bounds of the differential operator in the ratio of linear convergence. The latter provides a priori mesh independent estimates for the FEM realization and is due to the above-mentioned Sobolev space preconditioning background.

Besides the GFEM, we will sketch some other applications of Laplacian preconditioners. In the comparison to other numerical methods it is important to refer to Newton's method, widespread for its fast convergence. The problem of only local convergence and the extra work of compiling the Jacobians may justify the choice of a theoretically slower method, cf. e.g. [3]. In the GFEM the auxiliary linear problems are of fixed (Poisson) type, hence the matrices need not be updated in each step. Further, as we will see, in our problem the rate of linear convergence is suitably small. We note that for problems where the Laplacian preconditioner cannot yield a favourable ratio of convergence, one can still use the Sobolev space setting to construct preconditioned Newton iterations [4, 16, 25]. Some further remarks on the comparison of the GFEM, the nonlinear CGM and Newton's method will be given in Subsection 4.2.

The paper is organized as follows. Section 2 describes the physical model based on [12]. In Section 3 mathematical background is given. Section 4 is devoted to the construction and error estimate of the GFEM and some related applications of Laplacian preconditioners. Finally, in Section 5 numerical realization is developed for computing the tangential stress in a copper bar when crack occurs.

2. The physical model of 2D elasto-plastic torsion

The mathematical model of plastic state under plane deformation conditions was first given by Saint-Venant, and was later extended by von Mises to 3D, having a simple physical interpretation and structure.

In the hardening state the model of elasto-plastic torsion is given below following the presentation of Kachanov [12]. This model is based on the observation that the equations of deformation theory may be used for plastic deformations which develop in some definite direction. Since the tangential stress vectors act in parallel cross-sections, the model reduces the 3D problem to 2D.

We consider a hardening rod with cross-section $\Omega \subset \mathbf{R}^2$, the lower end of the rod being clamped in the (x, y)-plane. Our aim is to determine the tangential stress in the points of the rod under given torsion.

In the notations of this chapter, coordinates are denoted by subscripts and partial derivatives are denoted by $\frac{\partial}{\partial x}$ etc.

2.1. The Saint Venant model of torsion. In the Saint Venant model we assume that the cross-sections experience rigid rotation in their planes and are distorted in the direction of the z-axis. Denoting by $\omega > 0$ the torsion per unit length of the rod, the displacements u_x, u_y and u_z are then given by

$$(1) \qquad u_x = -\omega z y, \quad u_y = \omega z x, \quad u_z = w(x, y, \omega),$$

where w is an unknown function. Denoting as usual the components of shear strain by $\gamma_{xy}, \gamma_{xz}, \gamma_{yz}$, we obtain

$$\gamma_{xy} = \frac{\partial u_x}{\partial y} + \frac{\partial u_y}{\partial x} = 0,$$

$$(2) \qquad \gamma_{xz} = \frac{\partial u_x}{\partial z} + \frac{\partial u_z}{\partial x} = \frac{\partial w}{\partial x} - \omega y, \quad \gamma_{yz} = \frac{\partial u_y}{\partial z} + \frac{\partial u_z}{\partial y} = \frac{\partial w}{\partial y} + \omega x.$$

The tangential stress vectors τ also act in cross-sections parallel to the (x, y)-plane, i.e., denoting by τ_{xz} and τ_{yz} the x and y coordinates of τ, respectively, we can neglect the third coordinate and write

$$\tau = (\tau_{xz}, \tau_{yz}).$$

An important quantity, involving the tangential stress, is the twisting moment

$$(3) \qquad M = \int_\Omega (x\tau_{yz} - y\tau_{xz}) \, dx \, dy.$$

Further, the tangential stress satisfies the equilibrium equation

$$(4) \qquad \frac{\partial \tau_{xz}}{\partial x} + \frac{\partial \tau_{yz}}{\partial y} = 0.$$

Hence, we can introduce the stress function F fulfilling

$$(5) \qquad \tau_{xz} = \frac{\partial F}{\partial y}, \quad \tau_{yz} = -\frac{\partial F}{\partial x}.$$

The conditions (1) of rigid rotation in planes imply that the stresses in the rod are determined by those in the domain Ω. Further, the surface of the rod is free of normal stresses, hence the tangential derivative of F vanishes, i.e., we have

$$(6) \qquad F_{|\partial\Omega} \equiv const.$$

2.2. The hardening state. The condition of the hardening state involves the single curve model, wherein the connection between strain and stress depends only on strain and stress intensities

$$(7) \qquad \Gamma = \left(\gamma_{xz}^2 + \gamma_{yz}^2\right)^{1/2}, \quad T = \left(\tau_{xz}^2 + \tau_{yz}^2\right)^{1/2}.$$

Moreover, we require that T is a strictly increasing function of Γ. In the elastic state this function is linear owing to Hooke's law (i.e., $T = G\Gamma$, where $G > 0$ is Hooke's constant), then in the plastic state it becomes a concave nonlinear function. The stress-strain function is defined for arguments below a certain strain Γ_* (the end of validity of the elasto-plastic model), for which crack of the material first occurs.

The stress-strain function is usually written in the form

$$(8) \qquad\qquad T = g(\Gamma)\Gamma,$$

where the decreasing function g is called modulus of plasticity. The inverse is expressed in the similar product form

$$(9) \qquad\qquad \Gamma = \overline{g}(T)T.$$

According to the above, the increasing function $\overline{g}$ is also defined in a bounded validity interval $[0, T_*]$. Identities (8) or (9) are referred to as hardening condition.

2.3. The boundary value problem. The relations in (2) imply the continuity condition

$$(10) \qquad\qquad \frac{\partial \gamma_{yz}}{\partial x} - \frac{\partial \gamma_{xz}}{\partial y} = 2\omega.$$

Further, it follows from Hencky's relations that the strain and stress vectors are parallel, hence the hardening condition (9) yields

$$(11) \qquad\qquad \gamma_{xz} = \overline{g}(T)\tau_{xz}, \quad \gamma_{yz} = \overline{g}(T)\tau_{yz}.$$

Substituting this into (10) and using (5), we obtain

$$-\frac{\partial}{\partial x}\left(\overline{g}(T)\frac{\partial F}{\partial x}\right) - \frac{\partial}{\partial y}\left(\overline{g}(T)\frac{\partial F}{\partial y}\right) = 2\omega,$$

where

$$(12) \qquad T = \left(\tau_{xz}^2 + \tau_{yz}^2\right)^{1/2} = \left(\left(\frac{\partial F}{\partial x}\right)^2 + \left(\frac{\partial F}{\partial y}\right)^2\right)^{1/2}.$$

Since F is only determined up to an additive constant, the boundary value in (6) may be chosen 0. Hence the discussed model leads to the nonlinear boundary value problem written briefly as

$$(13) \qquad\qquad \begin{cases} -\mathrm{div}\left(\overline{g}(|\nabla F|)\nabla F\right) = 2\omega, \\ \qquad\qquad F_{|\partial\Omega} = 0. \end{cases}$$

If this is solved for F then the required tangential stress is obtained from (5).

2.4. Solution for a circular section. A special case when it is elementary to determine the tangential stress is a cylindrical rod, i.e., when the cross-section Ω is a disc. Then the symmetry yields $w = 0$ in (1), hence (2) gives

$$\gamma_{xz} = -\omega y, \quad \gamma_{yz} = \omega x, \quad \Gamma = \omega r,$$

where $r = (x^2 + y^2)^{1/2}$. Using parallelity as in (11), we obtain

$$(14) \qquad \tau_{xz} = g(\Gamma)\gamma_{xz} = -g(\omega r)\omega y, \quad \tau_{yz} = g(\Gamma)\gamma_{yz} = g(\omega r)\omega x.$$

In a general case for Ω, one has to apply a numerical method to determine the tangential stress.

3. Mathematical background

3.1. Sobolev space setting. For the investigation of the boundary value problem (13) we first introduce the operator

$$P(F) \equiv -\operatorname{div}(\overline{g}(|\nabla F|)\nabla F)$$

in the real Hilbert space $L^2(\Omega)$ with domain of definition $D(P) = H^2(\Omega) \cap H_0^1(\Omega)$. The function $\overline{g}$ is defined as in (9) in the validity interval $[0, T_*]$ and as constant $\overline{g}(T) \equiv \overline{g}(T_*)$ for $T \geq T_*$. Further, the conditions $\overline{g} \in C^1[0, \infty)$ and $\overline{g} > 0$, $\overline{g}' \geq 0$ are satisfied. The corresponding generalized differential operator $A : H_0^1(\Omega) \to H_0^1(\Omega)$ is defined by the identity

$$\langle A(F), V \rangle_{H_0^1(\Omega)} \equiv \int_\Omega \overline{g}(|\nabla F|)\nabla F \cdot \nabla V \, \mathrm{d}\Omega, \quad (F, V \in H_0^1(\Omega)),$$

where

$$(15) \qquad \langle F, V \rangle_{H_0^1(\Omega)} \equiv \int_\Omega \nabla F \cdot \nabla V \, \mathrm{d}\Omega$$

is the inner product on $H_0^1(\Omega)$ and $\mathrm{d}\Omega$ denotes the Lebesgue measure on Ω. Then the divergence theorem yields

$$\int_\Omega P(F)V \, \mathrm{d}\Omega = \langle A(F), V \rangle_{H_0^1(\Omega)} \quad (F, V \in H^2(\Omega) \cap H_0^1(\Omega)).$$

This, together with the identity

$$(16) \qquad \langle F, V \rangle_{H_0^1(\Omega)} = \int_\Omega (-\Delta F)V \, \mathrm{d}\Omega \quad (F, V \in H^2(\Omega) \cap H_0^1(\Omega)),$$

implies that

$$A_{|H^2(\Omega) \cap H_0^1(\Omega)} = (-\Delta)^{-1}P.$$

It can be verified in a usual way (see e.g. [19]) that A is Gâteaux differentiable and its derivative A' fulfils

$$\langle A'(F)V, V \rangle_{H_0^1(\Omega)} = \int_\Omega \Big(\overline{g}(|\nabla F|)|\nabla V|^2 + \frac{\overline{g}'(|\nabla F|)}{|\nabla F|}(\nabla F \cdot \nabla V)^2\Big)\mathrm{d}\Omega$$

for all $F, V \in H_0^1(\Omega)$. Hence (using the Cauchy-Schwarz inequality) A' satisfies

$$\int_\Omega \overline{g}(|\nabla F|)|\nabla V|^2 \mathrm{d}\Omega \leq \langle A'(F)V, V \rangle_{H_0^1(\Omega)} \leq$$

$$\int_\Omega \big(\overline{g}(|\nabla F|)|\nabla V|^2 + \overline{g}'(|\nabla F|)|\nabla F||\nabla V|^2\big)\mathrm{d}\Omega,$$

i.e., the uniform ellipticity property

$$(17) \qquad \lambda\|V\|_{H_0^1(\Omega)}^2 \leq \langle A'(F)V, V \rangle_{H_0^1(\Omega)} \leq \Lambda\|V\|_{H_0^1(\Omega)}^2 \quad (F, V \in H_0^1(\Omega))$$

holds with bounds

$$(18) \quad \lambda = \min_{T \geq 0} \overline{g}(T) = \overline{g}(0), \ \ \Lambda = \max_{T \geq 0}\{\overline{g}(T) + T\overline{g}'(T)\} = \overline{g}(T_*) + \max_{0 \leq T \leq T_*} T\overline{g}'(T).$$

The uniform ellipticity implies that A is uniformly monotone and Lipschitz continuous in $H_0^1(\Omega)$. This yields the existence and uniqueness (see e.g. [28]) for (13):

Theorem 3.1.   *Problem (13) has a unique weak solution* $F^* \in H_0^1(\Omega)$, *i.e.,*

$$\int_\Omega \overline{g}(|\nabla F^*|)\nabla F^* \cdot \nabla V \, \mathrm{d}\Omega = 2\omega \int_\Omega V \, \mathrm{d}\Omega \quad (V \in H_0^1(\Omega)).$$

3.2. Regularity. Although Theorem 3.1 guarantees the well-posedness of our problem (13), the weak solution has an insufficiency concerning the meaning of the model. Namely, for $F^* \in H_0^1(\Omega)$ it might occur in theory that $|\nabla F^*|$ is unbounded even for arbitrarily small ω. On the other hand, it is expected that the mathematical model is able to yield solutions whose derivatives are pointwise within the validity of the elasto-plastic model.

The following regularity result implies that indeed there exists

$$\max_{\overline{\Omega}} |\nabla F^*| \, < \, +\infty \, .$$

That is, problem (13) fulfils the above-mentioned requirement. Further, a higher regularity also holds in Sobolev sense.

Proposition 3.2 [18]**.**   *Let* $\Omega \subset \mathbf{R}^2$ *be a bounded domain with piecewise* C^2 *boundary, such that the angles at the corners are less than* π, *and* $\overline{g} \in C^1[0, \infty)$. *Then the weak solution of (13) satisfies* $F^* \in C^1(\overline{\Omega}) \cap H^2(\Omega)$.

(Incidentally, the result is formulated in [18] for a more general class, when $\overline{g}$ may depend on ∇F instead of $|\nabla F|$; further, the derivative of F is even Hölder continuous.)

4. Preconditioning by the Laplacian

Our aim is to determine the solution of (13) and its derivative. For this we investigate the numerical solution of the more general class of problems of the form

$$(19) \qquad \begin{cases} P(F) \equiv -\mathrm{div}\, g(x, \nabla F) = f(x), \\ \qquad\quad F_{|\partial\Omega} = 0 \end{cases}$$

that satisfy uniform ellipticity, i.e.,

$$(20) \qquad \lambda \|V\|_{H_0^1(\Omega)}^2 \le \langle A'(F)V, V \rangle_{H_0^1(\Omega)} \le \Lambda \|V\|_{H_0^1(\Omega)}^2 \quad (F, V \in H_0^1(\Omega))$$

with constants $\Lambda \ge \lambda > 0$, where $A : H_0^1(\Omega) \to H_0^1(\Omega)$ is the corresponding generalized differential operator, defined similarly to Subsection 3.1.

Our investigations are focused on a Sobolev gradient type iteration for problem (19). The main idea on the continuous level is that a steepest descent iteration is defined for the corresponding convex potential in the space $H_0^1(\Omega)$ under the H_0^1-inner product (15), further, a suitable regularity yields a constructive Sobolev gradient such that the iteration takes the form with Laplacian preconditioner

$$(21) \qquad\qquad F_{n+1} = F_n - \alpha_n(-\Delta)^{-1}(P(F_n) - f)$$

with some steplengths α_n. We will consider constant steplengths $\alpha_n \equiv 2/(\Lambda + \lambda)$, which are known to be optimal for an operator with bounds λ and Λ as in (20). The proposed numerical iteration is obtained as the projection of the theoretical sequence into a suitable FEM subspace (or sequence of subspaces).

The advantages of Laplacian preconditioners appear in two important areas. First, their efficiency for solving the auxiliary problems is justified by the various available fast Poisson solvers, see e.g. [24] and the references therein. Further, the

Laplacian as an elliptic operator is able to provide mesh independent convergence estimates.

In Subsection 4.1 the exact formulation of the construction and convergence of the GFEM is given, relying on the authors' earlier results in [9], where the gradient–finite element method (GFEM) has been introduced for the numerical solution of (19). In the GFEM the auxiliary linear Poisson equations, arising in (21), are solved by suitable FEM.

In Subsection 4.2 we sketch the nonlinear conjugate gradient method and inner-outer Newton iterations, where Laplacian preconditioning can be used with appropriate modifications of the GFEM setting.

4.1. Construction and convergence of the gradient–finite element method.
The GFEM has been defined in [9] by the following algorithm: let $(\delta_n) \subset \mathbf{R}^+$ be a sequence such that $\delta_n \to 0$. Then

$$(22) \qquad \left. \begin{aligned} &F_0 \in H^2(\Omega) \cap H_0^1(\Omega) \text{ is arbitrary;} \\ &\text{for any } n \in \mathbf{N}: \\ &(a)\ R_n = P(F_n) - f, \\ &\quad (Z_n^* = (-\Delta)^{-1} R_n \text{ denotes the exact solution} \\ &\qquad \text{of the auxiliary equation);} \\ &(b)\ Z_n \approx Z_n^* \text{ using FEM such that} \\ &\qquad Z_n \in H^2(\Omega) \cap H_0^1(\Omega) \text{ and } \|Z_n^* - Z_n\|_{H_0^1(\Omega)} \le \delta_n, \\ &(c)\ F_{n+1} = F_n - \frac{2}{\Lambda + \lambda} Z_n. \end{aligned} \right\}$$

In other words, Z_n is the numerically computed solution of the auxiliary Poisson equation

$$-\Delta Z = R_n, \quad Z_{|\partial\Omega} = 0,$$

using FEM with accuracy δ_n in $H_0^1(\Omega)$ norm.

Remark 4.1. The general form of the GFEM can be defined by allowing any $F_0 \in H_0^1(\Omega)$ and such that only $Z_n \in H_0^1(\Omega)$ is required. Then R_n is defined via the weak formulation of the operator P. We note that the convergence result cited below holds in the same way for the weak form of the GFEM. The strong form used in (22) that requires $Z_n \in H^2(\Omega) \cap H_0^1(\Omega)$ is motivated by qualitative aspects listed at the end of Subsection 5.2.

The convergence of the method is presented by the following theorem.

Theorem 4.1 ([9]). *Let the problem (19) fulfil the following conditions:*

(i) *The bounded domain $\Omega \subset \mathbf{R}^N$ is convex or fulfils $\partial\Omega \in C^2$; $g \in C^1(\overline{\Omega} \times \mathbf{R}^N; \mathbf{R}^N)$, $f \in L^2(\Omega)$.*

(ii) *The matrix $\frac{\partial g}{\partial p}(x, p)$ is symmetric, uniformly bounded and positive definite, i.e., there exist $\Lambda \ge \lambda > 0$ such that its eigenvalues are between λ and Λ for all $(x, p) \in \overline{\Omega} \times \mathbf{R}^N$.*

(iii) *There exists a constant $\gamma > 0$ such that $\left| \frac{\partial g_i}{\partial x_i}(x, p) \right| \le \gamma |p|$ for all $(x, p) \in \overline{\Omega} \times \mathbf{R}^N$.*

Let $0 < q < 1$ be fixed, $c_1 > 0$, $\delta_n \le c_1 q^n$ $(n \in \mathbf{N})$ and Λ as in (20). Then (with a suitable constant $c_2 > 0$) the following estimates hold for all n:

(a) *If $q > \dfrac{\Lambda - \lambda}{\Lambda + \lambda}$ then $\|F_n - F^*\|_{H_0^1(\Omega)} \le c_2 q^n$.*

(b)   If $q < \dfrac{\Lambda - \lambda}{\Lambda + \lambda}$ then $\|F_n - F^*\|_{H_0^1(\Omega)} \leq c_2 \left(\dfrac{\Lambda - \lambda}{\Lambda + \lambda} \right)^n$.

The proof relies on contractivity techniques (similarly as for any simple preconditioning method) and the ellipticity properties of the operator P regularized by the Laplacian.

Corollary 4.1.   *The GFEM converges as in Theorem 4.1 for the elasto-plastic torsion boundary value problem (13).*

Proof.   The class of problems (19) was introduced such that it contains (13). This is shown by the inequalities (17) and (20), which means equivalently that (13) fulfils conditions (i)-(iii) of Theorem 4.1. (Especially, we simply have $\gamma = 0$.)   □

The $H_0^1(\Omega)$ convergence of (F_n) implies the convergence of (∇F_n) to the required (∇F^*) in $L^2(\Omega)$ norm, where F^* is the unique weak solution of (19) applied as preconditioner in the inner iterations (cf. e.g. [25]). We underline that the resulting bound $(\Lambda - \lambda)/(\Lambda + \lambda)$ for the convergence quotient only depends on the original coefficient and is in this sense independent of the mesh size used.

Remark 4.2.   As mentioned in Remark 4.1, the above convergence result holds equally for the weak or strong form of the GFEM. However, the strong form has advantages in controlling the sequence of tolerances δ_n used in step (b) of (22). Namely, the sequence δ_n is strongly connected to the widths of the meshes h_n. Using the standard FEM error estimate, we have

$$\|Z_n - Z_n^*\|_{H_0^1(\Omega)} \leq Ch_n\|Z_n^*\|_{H^2(\Omega)} = Ch_n\|(-\Delta)^{-1}(P(F_n) - f)\|_{H^2(\Omega)} \leq$$

$$C'h_n\|P(F_n) - f\|_{L^2(\Omega)}$$

with suitable constants $C, C' > 0$. The obtained expression on the right-hand side plays the role of δ_n. If $(h_n) \to 0$ is chosen a geometric sequence and $\sup\{\|P(F_n) - f\|_{L^2(\Omega)} : n \in \mathbf{N}\} < +\infty$ (which can be assumed, since (F_n) is constructed to converge to the solution of equation $P(F) = f$), then the condition of Theorem 4.1 on δ_n is fulfilled, i.e. (instead of estimating δ_n in the steps) the suitably prescribed refinement of the mesh yields the required order estimate of the convergence of δ_n.

4.2. Some other iterations: conjugate gradients and inner-outer Newton iterations. In this subsection we sketch very briefly two other kinds of methods, where Laplacian preconditioning can be used with appropriate modifications of the previous considerations.

The Hilbert space version of the *nonlinear conjugate gradient method (CGM)* was introduced in [8] and extended to operators in a strong form in [15]. The Laplacian preconditioner used in the gradient–finite element method algorithm (22) can be equally applied for the CGM via a suitable modification of (22), using an auxiliary sequence (S_n) of conjugate directions defined simultaneously with (F_n). Namely, if R_n and Z_n are obtained in the same way as in (22), then the following steps are made:

(i) we calculate the constant $\gamma_n = -\alpha_n/\beta_n$, where

$$\alpha_n = \int_\Omega \frac{\partial g}{\partial p}(x, \nabla F_n)\, \nabla S_{n-1} \cdot \nabla Z_n \, \mathrm{d}\Omega, \qquad \beta_n = \int_\Omega \frac{\partial g}{\partial p}(x, \nabla F_n)\, \nabla S_{n-1} \cdot \nabla S_{n-1} \, \mathrm{d}\Omega;$$

(ii) we calculate the constant $c_n > 0$ as the smallest positive root of the equation

$$\int_\Omega g(x, \nabla F_n - c\nabla S_{n-1}) \cdot \nabla S_{n-1}\, \mathrm{d}\Omega \;=\; \int_\Omega f S_{n-1}\, \mathrm{d}\Omega;$$

(iii) we let

$$S_n = Z_n + \gamma_n S_{n-1} \quad \text{and} \quad F_{n+1} = F_n - c_n S_{n-1}\,.$$

The conjugate gradient method converges with ratio

$$\frac{\sqrt{\Lambda} - \sqrt{\lambda}}{\sqrt{\Lambda} + \sqrt{\lambda}}$$

[8, 15], hence the ratio obtained in Theorem 4.1 for the GFEM is improved. However, the price for this is the stepwise numerical integration for calculating the constants α_n, β_n and the numerical root search for finding c_n in each step of the iteration.

Another even more widespread way for the iterative solution of the nonlinear problem (19) is *Newton's method* (or its damped version). Its finite element realization can be easily constructed by projecting the Sobolev space Newton iteration into the considered FEM subspace (see, e.g., [4, 13, 23, 25]). This can be given by the following modification of the algorithm (22): instead of $Z_n^* = (-\Delta)^{-1} R_n$ defined there, we let

$$Z_n^* \;=\; L_n^{-1} R_n\,,$$

where L_n denotes the linearized elliptic operator at F_n:

$$L_n Z \equiv -\mathrm{div}\left(\frac{\partial g}{\partial p}(x, \nabla F_n)\, \nabla Z\right).$$

Then Z_n is the suitable FEM approximation of Z_n^* similarly as earlier. Further, we define the next iterate as

$$F_{n+1} \;=\; F_n + \tau_n Z_n\,,$$

where $\tau_n = 1$ in the original Newton's method and $0 < \tau_n \le 1$ is a suitable damping parameter in the damped version. For the convergence of Newton's method we assume the Lipschitz (or at least Hölder) continuity of $\partial g/\partial p$. This is inherited by the discretized nonlinear elliptic operator in any fixed finite dimensional FEM subspace $V_h \subset H_0^1(\Omega)$, hence one can prove in a standard way the corresponding superlinear convergence estimates, which are global in the case of suitable damping (see, e.g., [1] for details). For a study on the use of varied mesh sizes $h_n \to 0$ (the so-called multilevel Newton methods) see [5].

Finding the functions Z_n requires the FEM solution of general elliptic problems with the operators L_n, hence (in contrast to the Poisson equations in the GFEM algorithm) one can no more rely on any fast solver for these linearized equations and hence the work of their solution is no more negligable. Therefore, a much widespread way of solving the linearized equations is to apply distinct inner iterations for each of these equations. (These are generally preconditioned CG iterations, whose standard implementation for linear systems is found in [2].) In order to preserve the benefit of fast Poisson solvers, the discrete Laplacian might also be applied as preconditioner in the inner iterations (cf. e.g. [25]). The resulting convergence quotient is bounded by $(\Lambda - \lambda)/(\Lambda + \lambda)$ for a simple (Richardson) inner iteration and by $(\sqrt{\Lambda} - \sqrt{\lambda})/(\sqrt{\Lambda} + \sqrt{\lambda})$ for an inner CG iteration. These bounds only depend on the original coefficient and hence are mesh independent even if a multilevel

Newton's method is used. Regarding the convergence of the overall inner-outer iteration, we remark that Laplacian preconditioners yield an overall iteration which consists of Poisson equations just as well as the GFEM iteration (22), hence the stepwise contractivity bounds are the same. Therefore, it is easily seen that the order of required number of iterations to achieve a prescribed error is also the same as for the GFEM iteration, namely, $n = O(\log \varepsilon)$ as the prescribed error ε tends to 0.

5. Numerical solution of the elasto-plastic torsion problem

In the preceding sections it has been shown that determining the tangential stress requires the solution of the boundary value problem (13) for the stress function F.

From this we obtain the coordinates of the tangential stress according to the relations

$$(23) \qquad \tau_{xz} = \frac{\partial F}{\partial y}, \quad \tau_{yz} = -\frac{\partial F}{\partial x}.$$

For the numerical solution of the above boundary value problem we have introduced the gradient–finite element method, which exhibits linear convergence in $H_0^1(\Omega)$ norm.

This section is devoted to the investigation of the elasto-plastic torsion of a copper rod having square cross-section 10 mm × 10 mm. The purpose is to determine the tangential stress in the case of a torsion per unit slightly above the critical value, i.e., when crack occurs at the edge of the cross-section. (We use N for force and, for convenience, mm for length throughout the experiment.)

5.1. Determining the strain-stress function. The single curve hypothesis of the hardening condition implies that the connection of strain and stress can be determined from experiments with simple tension and pure shear [12]. This means that the strain-stress function is obtained directly, which is usual in the study of load elongation (e.g., work hardening of the compound AlZnMg [17]).

Another possibility is to measure the twisting moment (defined in (3)) versus the torsion per unit ω. This measurement has been achieved for copper cylinder [27]. The material was heat treated at the temperature 600°C for 1 hour. For the investigation of the mathematical model we need the strain-stress function $\bar{g}$ in the boundary value problem. Since the studied rod had a circular cross-section, the measurements of the moment enable us to determine the modulus of plasticity g as formulated below. From g we can obtain $\bar{g}$ using formulas (8) and (9).

Proposition 5.1. *Consider a rod with circular cross-section with radius a. Let the connection between the twisting moment and the twist per unit be given by the differentiable function $M = \Phi(\omega)$. Then we have*

$$g(\Gamma) = \frac{1}{2\pi a^4} \left(\frac{3a}{\Gamma} \Phi(\frac{\Gamma}{a}) + \Phi'(\frac{\Gamma}{a}) \right).$$

Proof.   From (3) and (14) we have

$$\Phi(\omega) = 2\pi\omega \int_0^a g(\omega r) r^3 dr = \frac{2\pi a^4}{\omega^3} \int_0^\omega g(at) t^3 dt.$$

Then suitable arrangement and differentiation yield the required statement.   □

Using the above formula, we obtain the following data from the measurements of [27]:

T	0	1.0779	1.2962	1.5238	1.7395	1.9293
$\overline{g}(T)$	1.0840	1.0840	1.1479	1.2160	1.2754	1.3201
T	2.5097	2.6786	3.4842	3.6339	4.0616	4.4678
$\overline{g}(T)$	1.4329	1.4650	1.6292	1.6614	1.7462	1.8166

T	4.5887	4.9247	4.9866	5.1473	5.3245
$\overline{g}(T)$	1.8486	1.9398	1.9811	2.0541	2.1259

Table 1.   The values of T mean $10^2 \times$ N/mm^2, and this will be used throughout the experiment. The values of $\overline{g}(T)$ mean $10^{-4} \times$ mm^2/N.

In the sequel the values of $\overline{g}(T)$ are determined by suitable interpolation using Table 1. Letting

$$T_* = 5.3245,$$

the validity interval is $[0, T_*]$ (see Subsection 2.2). The two cases $0 \le T \le 1.0779$ (with $\overline{g}(T) \equiv 1.0840$) and $1.0779 \le T \le 5.3245$ correspond to the elastic and plastic state, respectively.

5.2. Numerical realization of the GFEM. As can be seen in Theorem 4.1, the GFEM exhibits easy algorithmization and preserves the ellipticity bounds of the differential operator in the ratio of the global linear convergence. Further, we solve auxiliary linear problems of fixed (Poisson) type, hence (in contrast to Newton's method) the matrices need not be updated in each step. The realization of the GFEM requires a suitable FEM for these auxiliary Poisson problems.

The algorithm (22) has been defined involving the solution of the auxiliary problems in H^2. This approach requires the use of C^1 finite elements. (Although an intermediate degree between C^0 and C^1 might also be considered, see e.g. [29], in our case it is recommended to use C^1-elements for several reasons, discussed at the end of the subsection.) Therefore we use standard full quintic finite element approximation on each triangle. Then the 21 coefficients of the polynomials of degree 5 are determined such that 18 come from the values v, v_x, v_y, v_{xx}, v_{xy}, v_{yy} at the vertices and the remaining three from the normal derivatives v_n at the midpoint of each edge ([26]).

For the case $u^* \in H^k(\Omega)$ ($k = 1, ..., 6$), the error estimate ([26]) corresponding to this finite element subspace is

(24) $$\|u^* - u_h\|_1 \le const. \cdot h^{k-1} \|u^*\|_k .$$

It is worth underlining the case when u^* happens to be in $H^6(\Omega)$:

$$\|u^* - u_h\|_1 \le const. \cdot h^5 \|u^*\|_6 .$$

Remark 5.2.   (Reasons that justify C^1-elements.)   As is clear, the described higher order approximation leads to more arithmetic operations. However, the reasonability of its usage in general is presented in literature, in particular, it is also a basis for the hp-version (see e.g. [6, 29]). On the other hand, there are several aspects that especially justify this extra work in our case:

- According to Remark 4.1, the suitably prescribed refinement of the mesh yields the required order estimate of the convergence of GFEM. The usage of lower order elements would yield reduction of order; especially, in the case of C^0-elements the width h would not even appear in this estimate.
- The estimate (24) allows much coarser mesh to achieve prescribed accuracy.

- Using C^1-elements means finding the numerical solution in $C^1(\overline{\Omega}) \cap H^2(\Omega)$. This is favourable from qualitative point of view, since, according to Proposition 3.2, the smoothness of the solution is thus preserved.

5.3. Experiment. As mentioned above, first we wish to determine a torsion per unit ω for which the solution of problem (13) slightly increases above the critical state. This means that the modulus of the derivative of the solution (the stress intensity defined by (12)) slightly exceeds the maximum $T_* = 5.3245$ of the validity interval in some points of the cross-section, i.e., crack occurs.

Our aim, i.e., to determine the tangential stress field corresponding to the above value of ω, is achieved in the second step. Here the cross-section can be divided into three parts: elastic state, plastic state and where the crack occurs.

The numerical solution is carried out following Subsection 4.2. According to (18) in Subsection 3.1, the strain-stress function obtained above gives the ellipticity bounds

$$\lambda = 1.0840, \quad \Lambda = 4.6861.$$

From this the stepsize and the convergence quotient are

$$\frac{2}{\Lambda + \lambda} = 0.3466, \quad \frac{\Lambda - \lambda}{\Lambda + \lambda} = 0.6243.$$

Our principle for the stopping criterion relies, as usual, on the difference of consecutive terms. Namely, in each step we compute the nodal errors ε_n, which we define as the difference of the derivatives with respect to the mesh points. (Computing the nodal error requires no extra work, since the used values of derivatives appear during the FEM calculations.) When ε_n decreases below 10^{-4}, we also compute the error $e_n = \|F_n - F_{n-1}\|_{H_0^1(\Omega)}$ with numerical integration of suitably higher accuracy than for ε_n.

Computations are executed up to accuracy 10^{-4}. The FEM error estimate (24) shows that even $h = 2.5$ mm is a reasonable choice for this purpose. The convenience of this coarse mesh is due to the use of C^1-elements.

The experiments were carried out in the following way. In each step we computed the stress intensity $|\nabla F_n|$. We made some preliminary runnings for different values of ω. In order to reduce the computational cost, this was executed using coarser mesh ($h = 5$ mm). The results showed that the computed stress intensities $T_n := |\nabla F_n|$ stabilized in 3-4 steps around a value depending on ω. When this value arrived sufficiently close to T_*, we chose the corresponding torsion per unit $\omega = 0.3613$ mm^{-1} for the final running on the finer mesh.

We first give the results of the experiment with $\omega = 0.3613$ mm^{-1} and $h = 5$ mm in Table 2. The number of iterations n, the computed stress intensities T_n and the nodal errors ε_n are given.

n	1	2	3	4	5
T_n	3.4220	5.0535	5.3806	5.3888	5.3459
ε_n	1.8541	0.9439	0.2677	0.1336	0.1441

Table 2. Results with $\omega = 0.3613$ mm^{-1} and $h = 5$ mm.

This shows that the value, around which T_n is stabilized, lies slightly above T_*. This suggests that this ω is suitable for the final computations for the tangential stress.

In Table 3 we summarize the results of the computations with $\omega = 0.3613$ mm^{-1} and $h = 2.5$ mm. The required stopping criterion is $\varepsilon_n \leq 10^{-4}$.

n	1	2	3	4	5	6	7	8
T_n	3.4402	5.2090	5.4735	5.3440	5.4500	5.4040	5.4325	5.4174
ε_n	1.6552	0.8993	0.2487	0.0748	0.0423	0.0143	0.0088	0.0047
n	9	10	11	12	13	14	15	16
T_n	5.4237	5.4210	5.4226	5.4217	5.4223	5.4216	5.4219	5.4217
ε_n	0.0033	0.0018	0.0014	0.0010	0.0007	0.0004	0.0002	0.0001

Table 3.   Results with $\omega = 0.3613$ mm^{-1} and $h = 2.5$ mm.

After step 16 we computed e_{16}, using numerical integration of the gradients on a 20×20 mesh, and obtained $e_{16} = 0.000086$. Further refinement to 40×40 yielded $e_{16} = 0.000089$. The obtained values strengthen the reliability of the nodal stopping criterion. Consequently, we accept

$$\tilde{F} = F_{16}$$

as the numerical solution.

The surface and contours of the obtained tangential stress intensity are plotted in Figures 1 and 2, respectively. Here the cross-section can be divided into three parts: the corners and a small central part are in elastic state, in the middle of the edges crack occurs, and the intermediate region is in plastic state. This is shown by Figure 3.
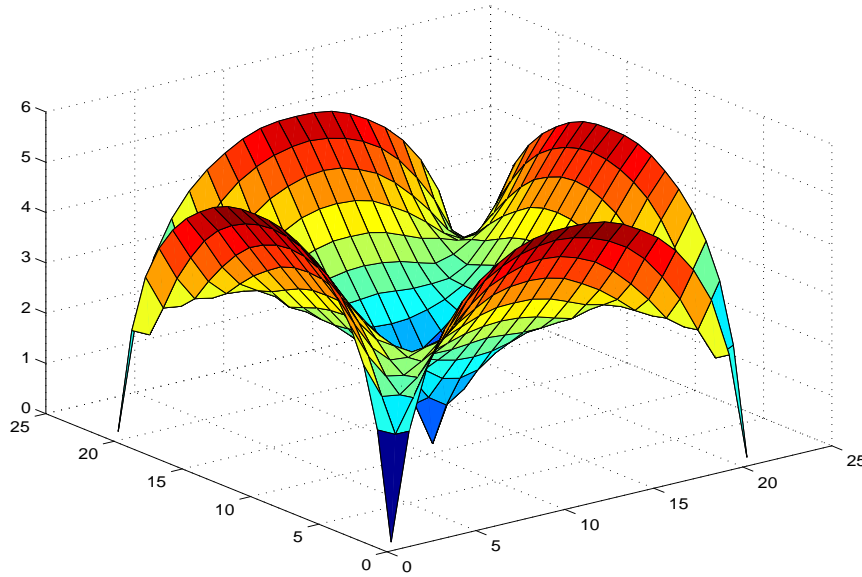
FIGURE 1. The surface of the tangential stress intensity

Remark 5.2.   Owing to the used C^1-elements, the numerically computed stress intensity $\tilde{T} = |\nabla \tilde{F}|$ is continuous. Therefore, its level contours are connected as well as those belonging to the exact solution. This would not be satisfied if lower order elements had been used. The latter may cause inconvenience when the contours are of interest, since in the discontinuous case they are disconnected.
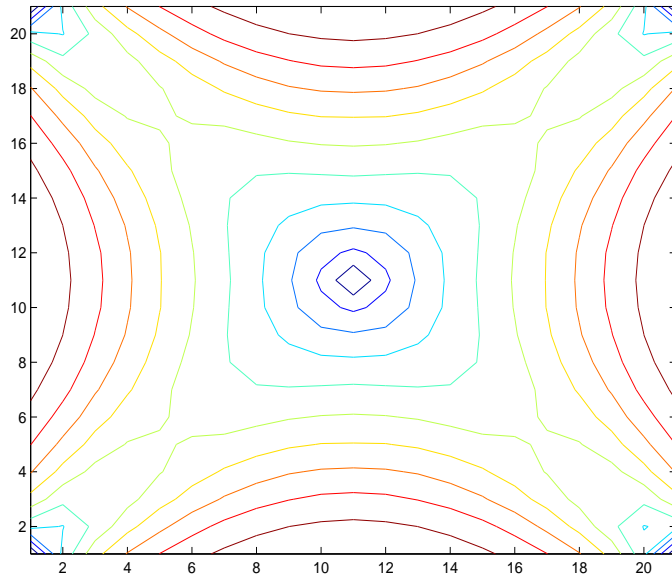
FIGURE 2. The contours of the tangential stress intensity
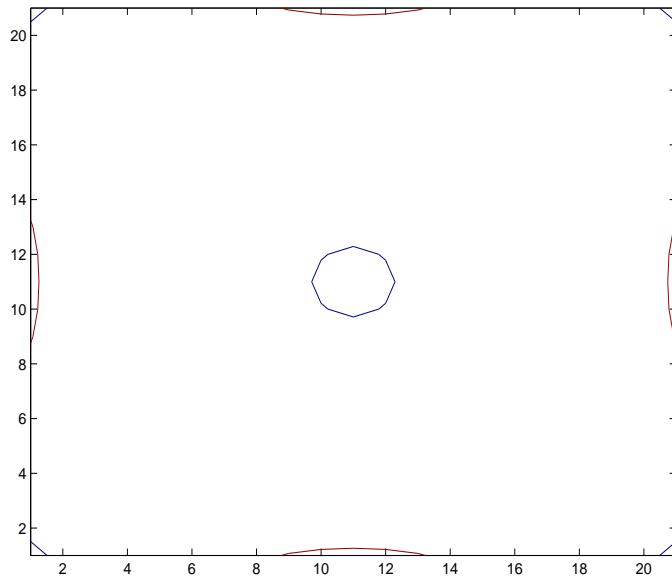
FIGURE 3. The regions of elastic state, plastic state and crack

5.4. Conclusion of the experiment. In this section we have investigated the elasto-plastic torsion of a copper rod, having cross-section 10 mm × 10 mm, in the hardening state. We have determined numerically the tangential stress in cross-sections under a torsion in the neighbourhood of the critical one when crack occurs. The iterative solution of the involved BVP has been achieved using the GFEM, and the properties of this method have been presented. Owing to the used C^1-elements,

the GFEM is a qualitatively reliable numerical method, since it preserves the continuity of the exact stress intensity and the corresponding connected contours of its modulus. According to the results, when slightly less than 0.3613 rad/mm (i.e. a little more than half rotation per cm) is executed then we can already experience crack in the material. The tangential stress intensities imply that the crack occurs in the middle of the edges, the central part of the cross-section is in elastic state, the intermediate region is in plastic state. This phenomenon corresponds to other results with different nonlinearity and numerical approach (see e.g. [12]).

Acknowledgments

References

[1] AXELSSON, O., On global convergence of iterative methods, in: *Iterative solution of nonlinear systems of equations*, pp. 1–19, Lecture Notes in Math. 953, Springer, 1982.

[2] AXELSSON, O., *Iterative solution methods,* Cambridge Univ. Press, 1994.

[3] AXELSSON, O., KARÁTSON J., Double Sobolev gradient preconditioning for elliptic problems, to appear in *Numer. Methods Partial Differential Equations.*

[4] AXELSSON, O., FARAGÓ I., KARÁTSON J., Sobolev space preconditioning for Newton's method using domain decomposition, *Numer. Lin. Alg. Appl.*, 9 (2002), 585-598.

[5] BLAHETA, R., Multilevel Newton methods for nonlinear problems with applications to elasticity, Copernicus 940820, Technical report.

[6] BORNEMANN, F.A., ERDMANN, B., KORNHUBER, R., A posteriori error estimates for elliptic problems in two and three space dimensions, *SIAM J. Numer. Anal.* 33 (1996), no. 3, 1188–1204.

[7] CAREY, G.F., JIANG, B.-N., Nonlinear preconditioned conjugate gradient and least-squares finite elements, *Comput. Methods Appl. Mech. Engrg.*, 62 (1987), No.2, pp. 145–154.

[8] DANIEL, J.W., The conjugate gradient method for linear and nonlinear operator equations, *SIAM J. Numer. Anal.*, 4 (1967), 10–26.

[9] FARAGÓ, I., KARÁTSON, J., The gradient–finite element method for elliptic problems, *Comput. Math. Appl.* 42 (2001), 1043–1053.

[10] FARAGÓ, I., KARÁTSON, J., *Numerical solution of nonlinear elliptic problems via preconditioning operators (Theory and applications)*, NOVA Science Publishers, New York, 2002.

[11] HAN, W., REDDY, B.D., *Plasticity. Mathematical theory and numerical analysis.* Interdisciplinary Applied Mathematics 9, Springer, 1999.

[12] KACHANOV, L.M., *Foundations of the theory of plasticity,* North-Holland, 1971.

[13] KANTOROVICH, L.V., AKILOV, G.P., *Functional Analysis,* Pergamon Press, 1982.

[14] KARÁTSON, J., The gradient method for non-differentiable operators in product Hilbert spaces and applications to elliptic systems of quasilinear differential equations, *J. Applied Analysis*, 3 (1997) No.2., 205–217.

[15] KARÁTSON, J., The conjugate gradient method for a class of non-differentiable operators, *Annales Univ. Sci. ELTE*, 40 (1997), 121–130.

[16] KARÁTSON J., FARAGÓ I., Variable preconditioning via quasi-Newton methods for nonlinear problems in Hilbert space, *SIAM J. Numer. Anal.* 41 (2003), No. 4, 1242-1262.

[17] KOVÁCS, I., LENDVAI, J., VÖRÖS, G., Effect of precipitation structure on the work hardening process, *Materials Sci. Forum* Vols. 217-222 (1996), 1275–1280.

[18] MIERSEMANN, E., Quasilineare elliptische Differentialgleichungen zweiter Ordnung in mehrdimensionalen Gebieten mit Kegelspitzen, *Z. Anal. Anw.*, Bd. 2 (4) 1983, 361–365.

[19] MIKHLIN, S.G., *The numerical performance of variational methods,* Walters-Noordhoff, 1971.

[20] MIYOSHI, T., *Foundations of the numerical analysis of plasticity,* North-Holland Math. Studies 107, Lecture Notes in Numerical and Applied Analysis, North-Holland, 1985.

[21] NEUBERGER, J. W., *Sobolev gradients and differential equations*, Lecture Notes in Math., No. 1670, Springer, 1997.

[22] NEUBERGER, J. W., *Steepest descent for general systems of linear differential equations in Hilbert space*, Lecture Notes in Math., No. 1032, Springer, 1983.

[23] Rannacher, R., Suttmeier, F.-T., A posteriori error control in finite element methods via duality techniques: application to perfect plasticity, *Comput. Mech.*, 21 (1998), No.2, 123–133.

[24] Rossi, T., Toivanen, J., A parallel fast direct solver for block tridiagonal systems with separable matrices of arbitrary dimension, *SIAM J. Sci. Comput.* 20 (1999), no. 5, 1778–1796 (electronic).

[25] Rossi, T., Toivanen, J., Parallel fictitious domain method for a non-linear elliptic Neumann boundary value problem, *Numer. Linear Algebra Appl.* 6 (1999), no. 1, 51–60.

[26] Strang, G., Fix, G.J., *An Analysis of the Finite Element Method,* Prentice Hall, Englewood Cliffs, 1973.

[27] Vörös, G., personal communication.

[28] Zeidler, E., *Nonlinear functional analysis and its applications,* Springer, 1986.

[29] Ženíšek, A., *Nonlinear elliptic and evolution problems and their finite element approximations.* Computational Mathematics and Applications, Academic Press, Inc., London, 1990.

ELTE University, Department of Applied Analysis, H-1518 Budapest, Pf. 120, Hungary
E-mail: `faragois@cs.elte.hu` and `karatson@cs.elte.hu`